Low Power Phase Quantizing Demodulators for a Zero-IF Bluetooth Receiver

Sohrab Samadian[1], Ryoji Hayashi[2], Asad A. Abidi[1]

[1]University of California, Los Angeles
[2]Mitsubishi Electric Corp., Information Technology R&D Center, Japan

Abstract -- **This paper presents low-complexity detectors for a zero-IF Bluetooth receiver based on phase-domain A/D conversion. Complexity and power issues are addressed and a technique is used to reduce power and complexity at the same time. At E_b/N_o of 13 dB bit error rate of demodulators is 10^{-3}.**

I. Introduction

Bluetooth is a low-cost short-range radio link, facilitating ad-hoc connections between mobile and stationary communicating devices. Bluetooth can only achieve its objective of low cost through hardware simplicity. So far, low-IF receivers have been proposed for Bluetooth communicating systems [1]-[2]. However, direct conversion to zero IF is simpler in terms of number of building blocks, and therefore promises lower power consumption and cost. Direct conversion radios suffer from their specific problems [3]. The most important of them are DC offset due to self-mixing of LO signal in the process of non- zero LO feed-through in downconversion mixers, and $1/f$ noise of CMOS transistors in a CMOS technology.

One way to solve these problems is to remove the corrupted low-frequency spectrum of down converted GFSK by a highpass filter (HPF). There is an optimum cut-off frequency of such an HPF; too low a cut-off frequency might not remove enough $1/f$ noise, whereas too high a cut-off might remove a big chunk of precious signal's spectrum. Also, such a highpass filter must itself be simple. Using an ideal FM discriminator, simulations show that a first-order HPF (Fig. 1) with cut-off frequency of up to 19kHz does not degrade theoretical BER of the 1 MHz-wide Bluetooth signal centered at zero IF beyond 0.1%, the acceptable BER limit set by Bluetooth specifications [4].

Although a correlator is the ideal FM demodulator [5], in practice it is often supplanted by the simpler limiter-discriminator. The discriminator may be based on a delay line to sense a frequency shift on every symbol [6], or a flip-flop to sense phase reversals [7]. One or more zero crossings are essential to the function of either type of discriminator. Figure 2 shows a sample Bluetooth modulated waveform downconverted to zero IF in quadrature phases, along with the same waveform downconverted to a non-zero IF of 1 MHz. This IF is selected to illustrate the waveform more clearly. Practical Bluetooth receivers often use 2 MHz IF. Owing to the low FSK modulation index of 0.32, there are no zero crossings in either i(t) or q(t) over intervals as long as three symbols in this example. In general, there is no upper bound on the length of intervals with no zero crossing. Non-zero IF signal however, crosses zero in each symbol. Therefore, a new type of discriminator must be sought for zero-IF Bluetooth receiver.

All-analog detectors can consume a considerable amount of power, whereas all-digital detectors need power hungry multi-bit analog-to-digital converters. Lee and Kwon [8] present a method to detect low-index FSK modulation that exploits analog pre-processing, followed by digital detection using an array of limiters. Sometimes a mixed analog-digital approach can be the lowest power solution, when low- power digital circuits follow simple analog circuits that implement powerful signal conditioning, altogether avoiding a multi-bit *voltage* A/D converter. In this paper we present the implementation and measurement results from this class of demodulator applied to Bluetooth at zero IF. Then, we introduce a simplified version. The performance of both detectors will be compared with theoretical bounds.

II. Multi-phase Limiter Discriminator

Bluetooth waveform at zero IF can be represented as a vector in a two-dimensional plane whose phase is modulated by data, as shown in Fig. 3(a). Whenever the vector crosses horizontal or orthogonal axis, it introduces a zero crossing in q(t) or i(t) waveforms in time. Modulation index determines maximum magnitude of angle of rotation per symbol ($\Delta\theta_{max} = h.\pi$ where h is modulation index). For a low index, phase rotations over many symbols may be confined to one quadrant and no zero crossings may appear in i(t) and q(t), as shown in the example of Fig. 2. This can happen when h is less than 0.5. However, if the four quadrants are uniformly subdivided into many segments, then

0-7803-7694-3/03/$17.00 © 2003 IEEE

the vector may be guaranteed to cross at least one segment boundary every symbol (Fig. 3(b)).

As noted in [8], just as the i(t) and q(t) downconverted signals amount to projections of the vector phase along orthogonal principal axes (0 °,90 °,180 °,270 °), linear combinations of i(t) and q(t) waveforms with trigonometric weights will create projections of the received waveform along segment axes (I_k and Q_k). For a pair of orthogonal axes rotated by θ_k relative to the principal axes (Fig. 3(b)), the projections i, q and i_k, q_k are related as following in time:

$$\begin{aligned} i_k(t) &= \cos\theta_k \cdot i(t) + \sin\theta_k \cdot q(t) \\ q_k(t) &= -\sin\theta_k \cdot i(t) + \cos\theta_k \cdot q(t) \end{aligned} \quad (1)$$

As the phase of the received waveform traverses these axes, it trips zero crossing detectors (Fig. 4). The greater the number of axes, the higher the resolution of phase detection. Demodulator counts number of clockwise and counter-clockwise zero crossings over one symbol period, and based on sign of the net count makes a decision at the end of symbol period whether data is 0 or 1. System simulations show that to detect Bluetooth modulation with an error rate of at least 10^{-3} (maximum allowed in Bluetooth [4]), quadrants of the phase plane must be divided uniformly into at least 8 segments, as defined by orthogonal axis pairs with rotations:

$$\theta_k = \frac{\pi k}{2^{M+1}}, k = 0,1,\ldots, (2^M-1) \quad (2)$$

where M=3 (Fig. 3(b)). In an implementation, this arrangement needs 16 limiting amplifiers followed by 8 zero crossing detectors to sense and latch transitions across phase thresholds (Fig. 4). Linear combiners in Fig. 4 are simple analog gain stages and adders that create intermediate signals $i_k(t)$ and $q_k(t)$ as defined by equations (1).

Zero crossing detectors clock at a multiple of symbol rate (oversampling factor), resolving time axis with sufficient resolution to sense the relative zero crossings of i_k and q_k. Simulations show that a moderate oversampling rate of 6 times is sufficient. We term this arrangement a 4-bit *phase-domain A/D converter.* Zero crossings can be detected on small amplitude waveforms with a reasonable signal-to-noise ratio; there is no need for amplification by an AGC to some perfect large amplitude.

Now, let us compare this phase-domain demodulator with a linear (digital) FM discrimination on quadrature channels at zero IF. This discriminator consists of a PLL with a VCO whose outputs are in quadrature, and a phase detector that forms the cross product of the quadrature waveforms at the PLL input with the quadrature outputs of the VCO. We assume that prior to demodulation, and AGC loop amplifies the received signal to the full-scale of an A/D converter. The higher the resolution of this converter, the lower the error rate in detection. We explore this in simulation with quantizers of progressively higher resolutions. An oversampling of 64 times is used to eliminate any artifacts due to quantization in time. We find that for the FM demodulator to perform as well as the phase-quantizing approach, the input voltage waveforms must be quantized with a resolution of at least 5 bits (Fig. 5). Two parallel 5-bit converters in I and Q channels require a total of 64 comparators, whereas the phase quantizing approach needs only 16 and no AGC.

III. Simplification by Phase Encoding

Instead of sensing phase rotation by counting crossings across phase axes, it is possible to read the instantaneous phase by a 16-bit thermometer code at the output of comparator array in Fig. 6(a). With eight zero crossing detectors this code resolves the instantaneous phase to an accuracy of $\pi/16$. For example the code corresponding to the shaded segment in Fig. 6(b) is '0000 1111 1111 1111'. As the phase vector of GFSK signal rotates clockwise from shaded segment to the striped segment in Fig. 6(b), the code changes to '0000 0111 1111 1111' and if the vector rotates counter--clockwise to the dotted segment, the code becomes '0001 1111 1111 1111'. Now the demodulator need only look at the initial and final values of code over one symbol to extract the angle of the received waveform and its direction of rotation. This leads to a much simpler circuit (Fig. 7) compared to the earlier detector of Fig. 4 that counts zero-crossings. Although it is necessary to oversample the downconverted signal to synchronize timing, the detector itself clocks at symbol rate, 1 MHz, which lowers its power consumption.

Unlike most of other mobile wireless systems, Bluetooth terminals meant to connect, for instance, a PDA to a desktop computer over short ranges are not subject to high speeds. Data rate in Bluetooth is also rather low (1 Mb/sec.) and in this scenario there is no need to characterize Bluetooth demodulator in rapidly time-varying multipath channels.

IV. Experimental Results

The zero crossing demodulator (Fig. 4) was implemented on a Xilinx FPGA mounted on an XESS XS40 test board. The detector uses an equivalent of 470 NAND gates. Two synchronized arbitrary waveform generators synchro-

nize Bluetooth GFSK waveforms, modulated by random data, in quadrature phases at zero IF. Off-the-shelf analog components on a separate circuit board implement the trigonometric-weighted sums required to create projections on the intermediate phase axes according to equations (1). For data rate of 1 Mb/s specified by Bluetooth, this detector must clock at 6 MHz (oversampling factor = 6) to capture zero crossings with sufficient resolution.

The simplified demodulator (Fig. 7) implemented on the same FPGA uses only an equivalent of 60 NAND gates. This is mainly due to removing zero crossing detectors from demodulator. In addition, simplified detector clocks at symbol rate of 1 MHz, six times less than zero crossing demodulator.

Figure 8 shows BER measurement results from both detectors. The simplified demodulator is 0.5 to 1 dB more sensitive than the zero-crossing detector, because with a reasonable oversampling rate such as 6 zero-crossings are captured with a limited resolution on the time axis, which can induce errors. Both measurements lie close to bit-by-bit simulations of the detectors. As also shown in this figure, the detectors' characteristics lie close to a fully coherent 0.32-index CPFSK demodulator and bounded by the theoretical non-coherent demodulator of Bluetooth [9].

For an error rate of 10^{-3}, the highest allowed in Bluetooth, the detectors require an E_b/N_o of about 13 dB. Bluetooth specifies a minimum detectable signal of -70 dBm and a data rate of 1 Mb/sec.; then using the equation $Signal_{min} = -174 + 10 \log f_b + NF + E_b/N_{omin}$ we infer that the receiver noise figure (NF) must be less than 31 dB. It is relatively easy to implement a receiver which consumes a very small power and whose NF is well below this limit in today's technology.

V. Conclusion

This paper has described the problem of demodulating narrowband Bluetooth FSK signal centered at zero IF, and proposed two solutions. Both are based on a 4-bit phase domain A/D converter followed by simple logic circuits to detect signals in the presence of noise with adequate sensitivity for Bluetooth. A mixed signal implementation of these detectors is simple, compact, and low power. Measured results of BER versus SNR from experimental prototypes match closely to simulations, and are close to the characteristics of a fully coherent 0.32-index GFSK detector. Although discussed for Bluetooth, this class of demodulators can be used in any narrowband CPFSK standard.

References

[1] H. Darabi, *et al.*, "A 2.4 GHz CMOS transceiver for Bluetooth" in 2001 *IEEE JSSC*, vol. 36, no. 12, pp. 2016-2024.

[2] F.O. Eynde, *et al.*, "A fully integrated single-chip SOC for Bluetooth", in *2001 IEEE ISSCC*, pp. 196-7, 446.

[3] A. A. Abidi, "Direct-Conversion Radio Transceivers for Digital Communication", *IEEE Journal of Solid-State Circuits*, vol.30, no.12, pp. 1399-1410, 1995.

[4] "Specification of the Bluetooth System", ver.1.1, 2001.

[5] J. Proakis, *Digital Communications*. Mc Graw-Hill, 1995.

[6] H. Komurasaki, et al., "A single-chip 2.4 GHz RF transceiver LSI with a wide-range FV conversion", in *2001 IEEE ISSCC*, pp. 206-7, 448.

[7] I. A. W. Vance, "Fully Integrated Radio Paging Receiver", *IEE Proceedings*, vol. 129, Part F, no. 1, pp. 2-6, 1982.

[8] E. K. B. Lee and H. M. Kwon, "New baseband zero-crossing demodulator for wireless communications. I. Performance under static channel", in *MILCOM 95. Universal Communications*. San Diego, CA, USA, pp. 543-7 vol. 2, 1995.

[9] W. P. Osborne and M. B. Luntz, "Coherent and noncoherent detection of CPFSK", *IEEE Transactions on Communications*, vol. COM-22, no. 8, pp. 1023-36, 1974.

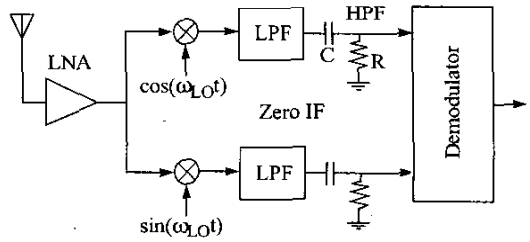

Figure 1. Block diagram of zero IF receiver. Low pass filter (LPF) removes adjacent channels, and R-C highpass filter (HPF) suppresses DC offset and $1/f$ noise of previous circuits.

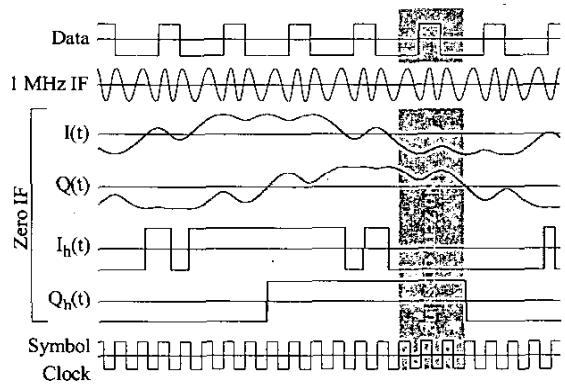

Figure 2. Comparing Bluetooth waveform at 1 MHz IF and at zero IF. There's no zero crossings in I and Q for 3 symbols although data is changing.

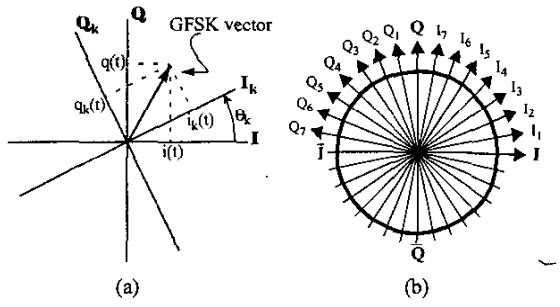

Figure 3. (a) Representation of Bluetooth phase vector and it's projection on I-Q axes and the rotated axes. (b) Rotated pair of I-Q axes segment each quadrant into eight sectors.

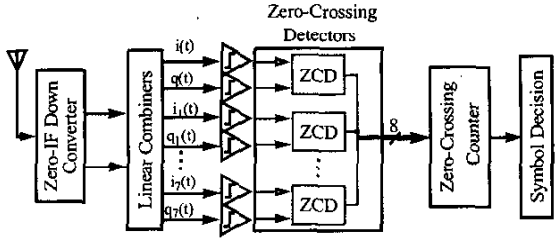

Figure 4. Block diagram of zero IF zero crossing demodulator

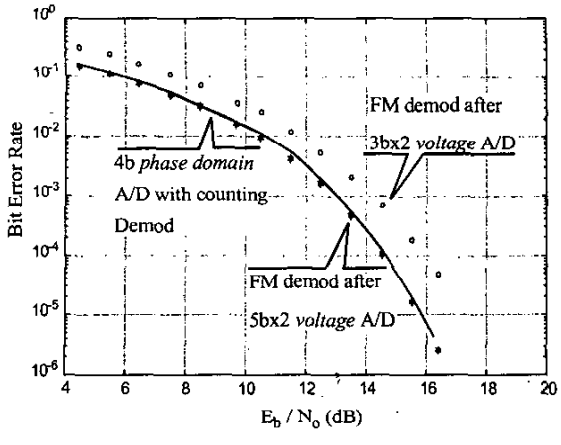

Figure 5. Comparing performance of new demodulator based on phase quantization (line) with ideal FM demodulator following voltage quantization of i(t) and q(t) waveforms to different resolutions (points).

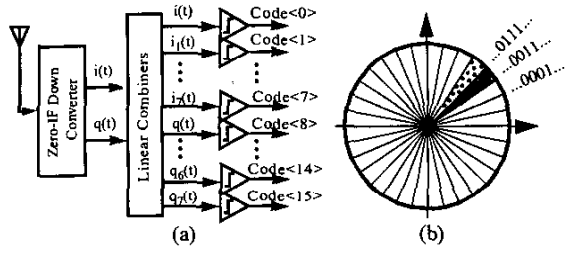

Figure 6. (a) Direct thermometer code readout from phase domain A/D converter. (b) Correspondence between code outputs and segments of phase.

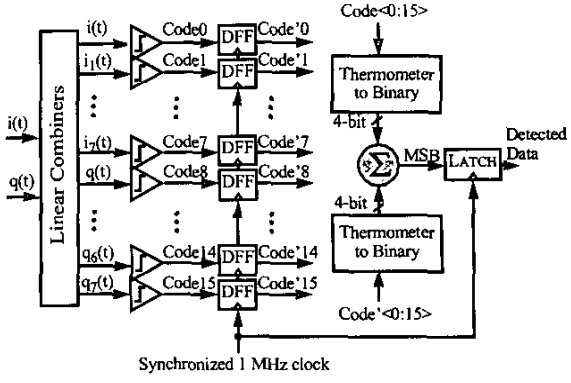

Figure 7. Block diagram of simplified demodulator

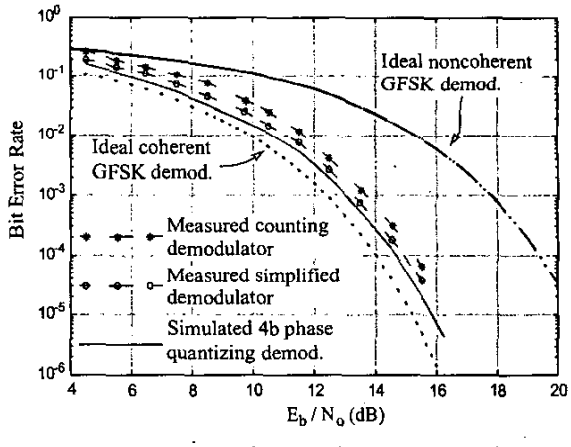

Figure 8. Measured performance from prototypes of both phase quantizing demodulators compared with simulation. Bounds imposed by ideal coherent and noncoherent 0.32-index GFSK detectors are also shown.